

Article

Mechanical and Corrosion Behavior of Al-Zn-Cr Family Alloys

Ahmed Nassef ¹, Waleed H. El-Garaihy ^{2,*} and Medhat El-Hadek ¹

¹ Department of Production & Mechanical Design, Faculty of Engineering, Port-Said University, Port Said 42526, Egypt; nassef12@eng.psu.edu.eg (A.N.); melhadek@eng.psu.edu.eg (M.E.)

² Mechanical Engineering Department, Unizah College of Engineering, Qassim University, Buraydah, Kingdom of Saudi Arabia

* Correspondence: W.Nasr@qu.edu.sa; Tel.: +966-55-110-8490

Abstract: Aluminum base alloys containing chromium (Cr) and zinc (Zn) were produced using extrusion and heat treated powder metallurgy. Cr addition ranged between 5 to 10 wt. % while Zn was added in an amount between 0 to 20 wt. %. Heat treatment processes were performed during powder metallurgy process at different temperatures followed by water quenching. Similar alloys were extruded, with an extrusion ratio of 4.6 to get proper densification. Optical microscopy was used for microstructure investigations of the produced alloys. The element distribution microstructure study was carried out using the Energy Dispersive X-ray analysis method. Hardness and tensile properties of the investigated alloys have been examined. Wear resistance tests were carried out and the results were compared with these of the Al-based bulk alloys. Results showed that the aluminum base alloys containing 10wt. % Chromium and heat treated at 500°C for one hour followed by water quenching exhibited the highest wear resistance and better mechanical properties.

Keywords: Al-Zn-Cr Alloys; powder metallurgy; strengthening; extrusion; dry sliding wear

1. Introduction

Aluminum matrix composites (AMC) have great potential in the transportation, electronic and leisure industry [1- 4]. The research and development in this area have been devoted to the process of optimization and the property determination of the aluminum (Al) composites containing additives [2]. The mechanical alloying techniques can produce amorphous, nanocrystalline and supersaturated alloy powders at low temperatures [3]. In mechanical alloying a mixture of different kinds of metal powders is mechanically alloyed near room temperature by compression, friction and shearing due to collision and rub of mill-balls. The large mechanical energies introduced into the powder particles are nanocrystalline interfaces, amorphous state, and promote reactions between the metals in solid state [5- 7]. Studies on the trinity Al-Zn-Cr alloys have been very limited through the literature. Recently Kurtuldu *et. al.* investigated the effect of trace additions on the aging behavior of aluminum alloys containing Cr and the effect of Cr addition on Zn diffusion in liquid Al-Zn-Cr alloys [8-9]. It is very interesting to notice that the minor and trace additives have a noticeable effect on these alloys as far as structure and tensile properties are concerned [10]. In view of the excellent corrosion and oxidation resistance, the strengthening and toughening of these alloys have been of recent interest [7- 11]. Running experiments on the Al-Cr-Zn system at 600 °C, eleven three phase regions had been identified [12]. Li *et. al.* studied the effect of grain structure on quench sensitivity of an Al-Zn-Mg-Cu-Cr alloy, the results showed that the decrease of the quenching rate from 960 °C/s to 2 °C/s revealed a decrease in the hardness after aging for the homogenized and solution heat treated alloy (H-alloy) with large equiaxed grains, for the extruded and solution heat treated alloy (E-alloy) an elongated grains and subgrains had been dominated [13]. The Al-based alloys with additives of magnesium (Mg), and silicon (Si) belong to wrought aluminum alloys which

are heat treated. It is worth mentioned that there is an increase in the mechanical strength of the alloys as long as there is an increase in Mg and Si to the solubility limits on the other hand the ductility will be reduced. Small amount of Mg, Cr, Zn, Zr, or Ti has, for a long time, been added to modify the microstructure in order to improve the mechanical properties, formability and corrosion resistance of the alloy [14-17]. Enhanced wear and corrosion resistance is considered to be one of the most important attributes of AMC that contain ceramic particles for engineering applications [18]. A progressive loss of materials occurs when two sliding surfaces come in contact and this process is known as wear. Such interaction between surfaces gives rise to friction. Wang studied the effect of additives as copper (Cu) and silicon carbide (SiC) on Al-based alloys [19]. Aluminum alloys matrices with particulate Al_2O_3 or SiC reinforcements possess higher strength and stiffness as well as greater wear resistance and improved high properties [20-21]. Studies considering other reinforcement particles, for example Cr, iron (Fe), and so on have been limited.

It was intended by the present work to control and optimize the production processing parameters through suitable die design compaction with dense powder metallurgy (PM) parts. Study the influence of the production methods, and chromium and zinc addition to aluminum alloys on the structure density, tensile behavior, hardness, corrosion and wear resistance of the Al-based alloys. Using cold pressed powder metallurgical process the alloys were manufactured with controlled alloy constitutions with heat treatment, and also with extruded conditions.

2. Materials and Methods

Because of the strong ionic interatomic bonding of Cr and Zn, desirable material characteristics are obtained. Powders with purity greater than 99% with an average particle size less than 50 μm in diameter and manufactured by CNPC powder-Canada were used as the starting source materials. The aluminum metallic powder was obtained from ALDRICH-Germany. Al-based alloys with different compositions were prepared using a mechanical mixer to achieve the planed composition. Six different compositions were prepared namely as, Al-5Cr, Al-7.5Cr, Al-10Cr, Al-20Zn, Al-20Zn-5Cr, and Al-20Zn-10Cr. Each powder mixture was then cold pressed using a compaction pressure of 425 MPa on the 30mm diameter billets. The material properties are expected to be diverse since the melting temperatures of Al is around 660°C, Cr is around 1900°C, and Zn is around 420°C. The powder density of Al is 7190 kg/m^3 , Cr is 2700 kg/m^3 , and Zn is 7140 kg/m^3 . After cold pressing the alloys were then heat treated to 500°C for duration of 60 minutes. Also, similar alloys were extruded, with an extrusion ratio of 4.6 to get proper densification. The behavior of the extruded alloy was studied. The extruded bars were subjected to solution treatment temperature of 500°C for 60 minutes and then quenched in room temperature water. As the size of the small particle with high curvature increase the differences in free energy across the curved surface increases as discussed [22-23].

3. Results and Discussion

3.1. Densification Behavior

The densification behavior of the investigated al-based alloys as affected by chromium, and zinc additions are shown in Figure 1. It is worth mentioned here that there is a direct proportionality between the alloys density and the sintering temperature. Three classes of mechanisms contribute to densification: plastic yielding, low power creep and various sorts of diffusion. In the absence of an external pressure, only the diffusion mechanisms exist as sintering is applied. Pore dragging and pore separation from the pores tend to inhabit the diffusion contribution. The rate equations are given in different publications [4, 7]. Theoretical solid densities normalized by after extrusion density of all produced parts are shown in Figure 2. Higher relative densities (RD) were achieved for hot extruding samples to around 99% from the solid density values. Zinc particles with its lubricating effect will enhance to a great extent the packing loss of the powders and will retard the

sealing for the individual pores. Consequently, density will decrease with zinc additions. This may be liquid zinc diffused inside the aluminum matrix and leaves pore inside the matrix. For the Al-based alloys, Cr particles were observed in the microstructure after heat treatment at 500°C for one hour followed by water quenching. No difference in the microstructures was observed for these alloys that are heated treated at 500°C for one hour followed by water quenching as shown in Figure 3. From the microstructures of the heat treated samples Al-5Cr homogeneous structure was observed at a temperature of 500°C followed by water quenching.

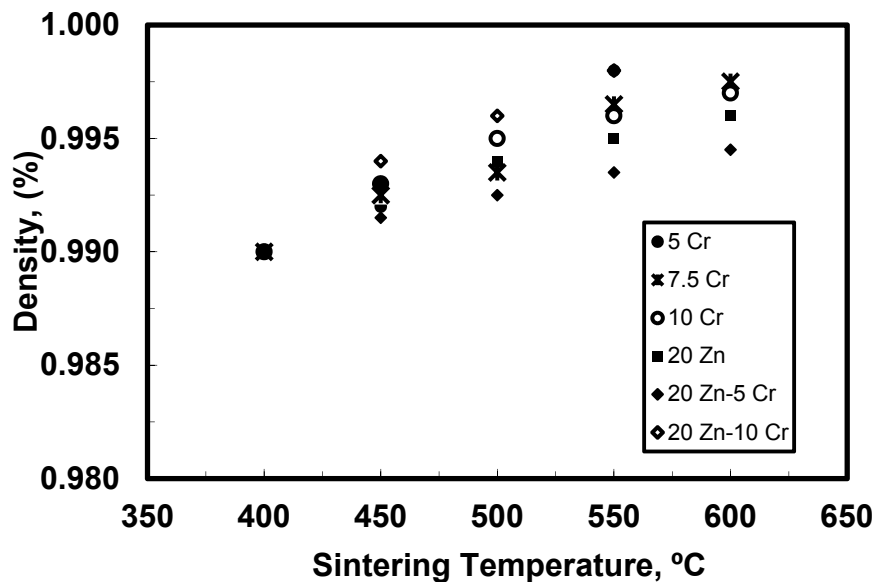


Figure 1. The effect of the sintering temperature on the density for different Al-base alloys.

3.2. Microstructural Optical Investigations

There is a difficulty in revealing the grain boundaries in Aluminum alloys especially under heat treatment conditions, so anodizing is required for the lower alloy content grades. Anodizing is electrolytic etching procedure that deposits a film on the specimen surface revealing the grain structure when viewed with crossed polarized light. Using either the Keller's reagent or the Grafet-Sargent reagent for the more highly alloyed grades could lead to etch them successfully.

The microstructure for Al-based alloys subjected to heat treatment temperature of 500°C for 60 minutes followed by quenching in water at room temperature as shown in Figures 3. As, the microstructure for Al-based alloys subjected to extrusion with an extrusion ratio of 4.6 with solution heat treatment temperature of 500°C for 60 minutes followed by quenching in water at room temperature as shown in Figures 4. The uniform distributions of the Al, Cr and Zn in the homogenous structures were noticed in alloys with Al-based alloys. Rapid growth of the grains during sintering was observed as one of the limitations of the cold pressed PM method as presented in figures (a - f). Also, it should be reported that surface cracks in the Al-based alloys were very limited. Increasing heating temperature for Al-20Zn alloys led to a considerable increase in the number of pores formed at high temperature, as the sample revealed sound. Homogenous microstructure with no pores is shown in Figure 3(d). Al-Zn-Cr alloys were used as a base for the ternary system. The Cr contents in this ternary system were investigated in Al-20Zn-5Cr and Al-20Zn-10Cr alloys. It is noticed in the micrographs of the extruded billet with heat treatment Figures 4 (a - f) that a fine dispersion of precipitates occurs on the grain surface.

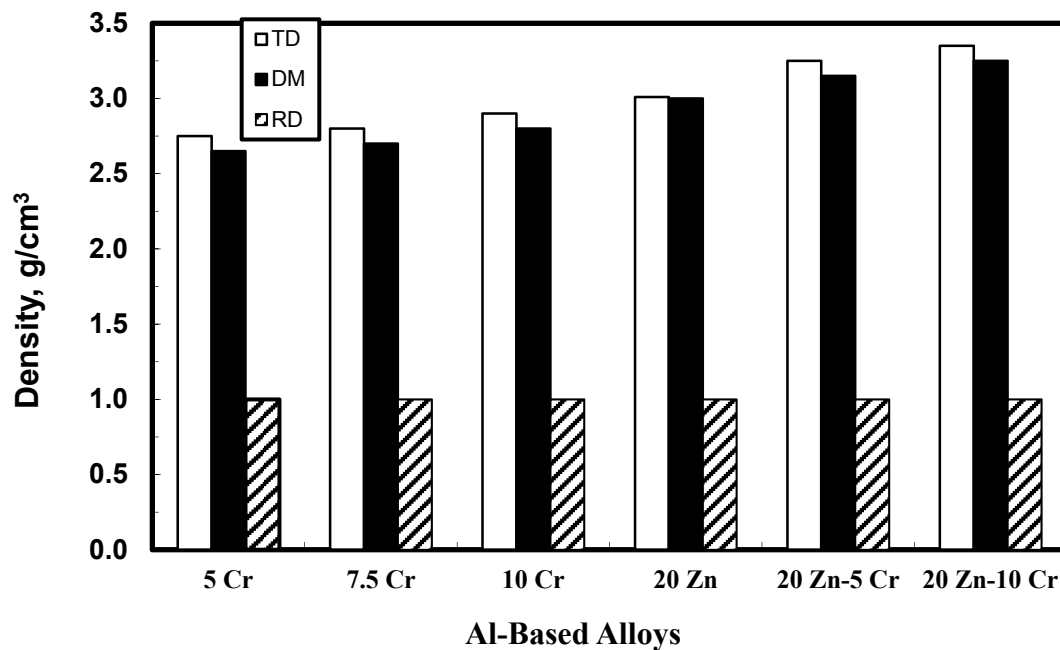


Figure 2. The density of as extruded Al-base alloys.

The formation of lots of finely distributed polygonal type of the Cr and Zn particles in the interface of liquid solid former during solidification may leads to refinement. The process reduces the porosity by the formation of necks between powders to achieve final elimination of the small pores at the end of the process. It forms new but lower energy solid-solid interfaces with a decrease in the free energy occurring on sintering one micrometer particles is a 1 cal/g decrease. On a microscopic scale, material transfer was affected by the change in the pressure and the differences in free energy across the curved surface. Multi-phases were observed in the microstructure in the as-extruded sample as shown in Figures 4 (e, and f).

The liquid phase was formed at the hot pressing temperature and consolidation was further enhanced by the isostatic action of the compressive stresses on the compact inside the dies [4, 7]. Additionally, diffusion rates were increased by the liquid phase and densification was enhanced by good wetting between liquid and solid components of the alloy system.

3.3. Energy dispersive X-ray (EDX) Analysis

The Al-based alloy samples for microscopic examination were prepared using the standard metallographic procedures and were examined at a magnification of 100X by scanning electron microscopy. Quantitative energy dispersed X-ray (EDX) analysis was also performed to analyze the element composition for the different heat treated samples.

After the fabrication process, a Jeol 5400 scanning electron microscope (SEM) unit with a link energy dispersive x-ray spectroscopy (EDS) detector is attached to observe the particle morphology, particle size, particle shape, and agglomeration of particles. Diffusion layers of chromium in aluminum occurred with decreasing chromium content from the center of these layers towards the matrix of the sample as shown in Figure 3(a). The EDX analysis emphasizes this behavior, as shown in Figure 5. The magnified attached to figures 5(e, and f) show that a white large phase was being embedded in a matrix of Al-Zn as seen from EDX analysis region, as the small white phases were mainly Zn particles. After heat treatment process mentioned above a more homogeneous structure was obtained. The magnified attached to figure 5(f) show a white and a dark area, the analysis of these areas was given as in EDX analysis region. It can be observed that the white area was Cr rich while the dark area was mainly Zn. Figure 3 (e, and f) shows micrographs of Al-20Zn-5Cr and

Al-20Zn-10Cr alloys, respectively, with heat treatment for one hour followed by water quenching. The liquid Zn during heating indicates homogenous structure as the Cr particles become smaller than before heating. It shows that the nucleus was enriched with the addition of Cr. The data from EDS spectrum shows that the nature of nucleus was facilitated as the foreign particle displays a small lattice mismatch in the al-based alloys. The results of calculation for some possible crystallographic orientations on the cr particles as the planar disregistry was the low, therefore Cr can act as the heterogeneous nucleation for the al-based alloys.

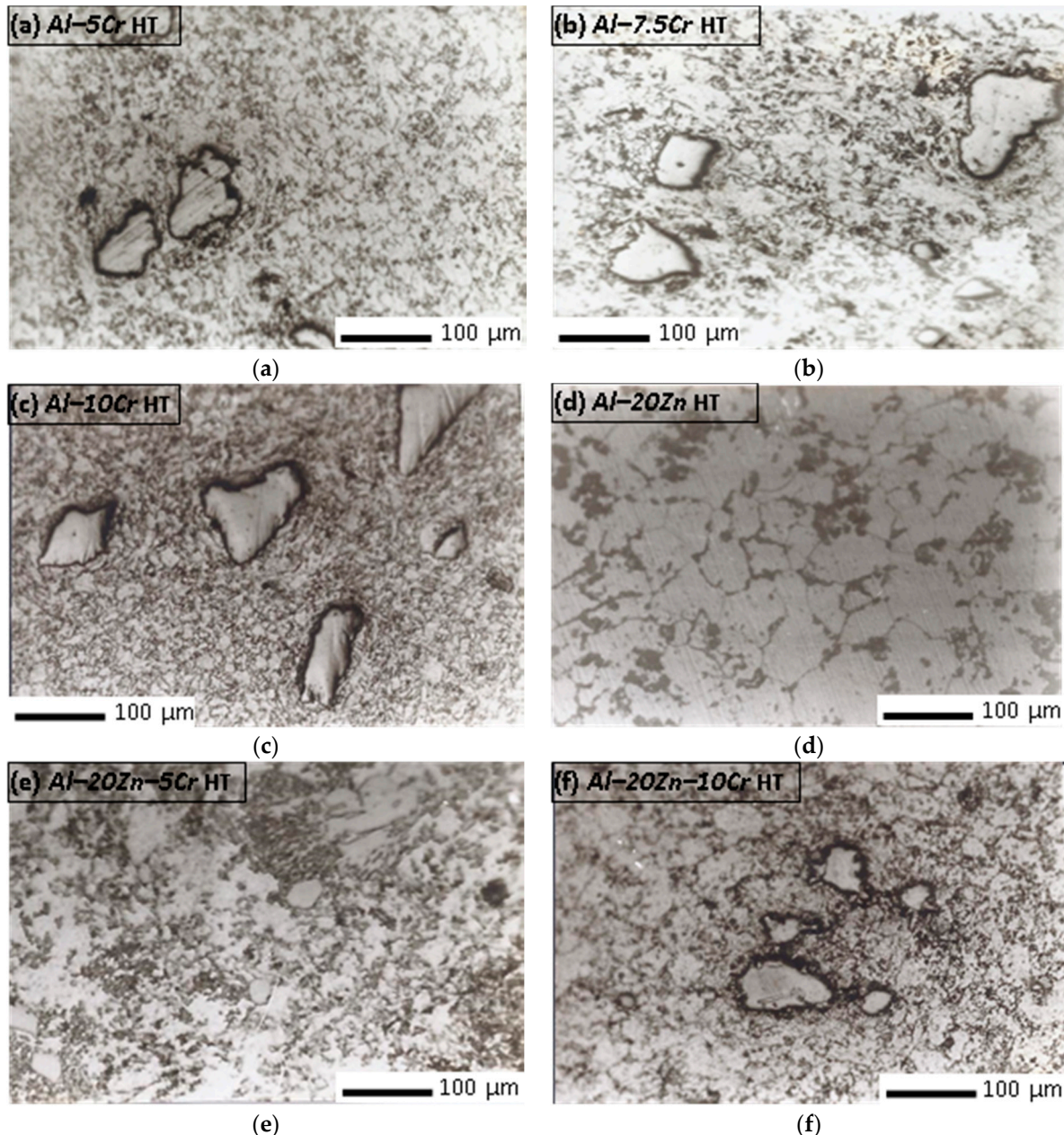


Figure 3. The microstructure of the different heat treated Al-based alloys.

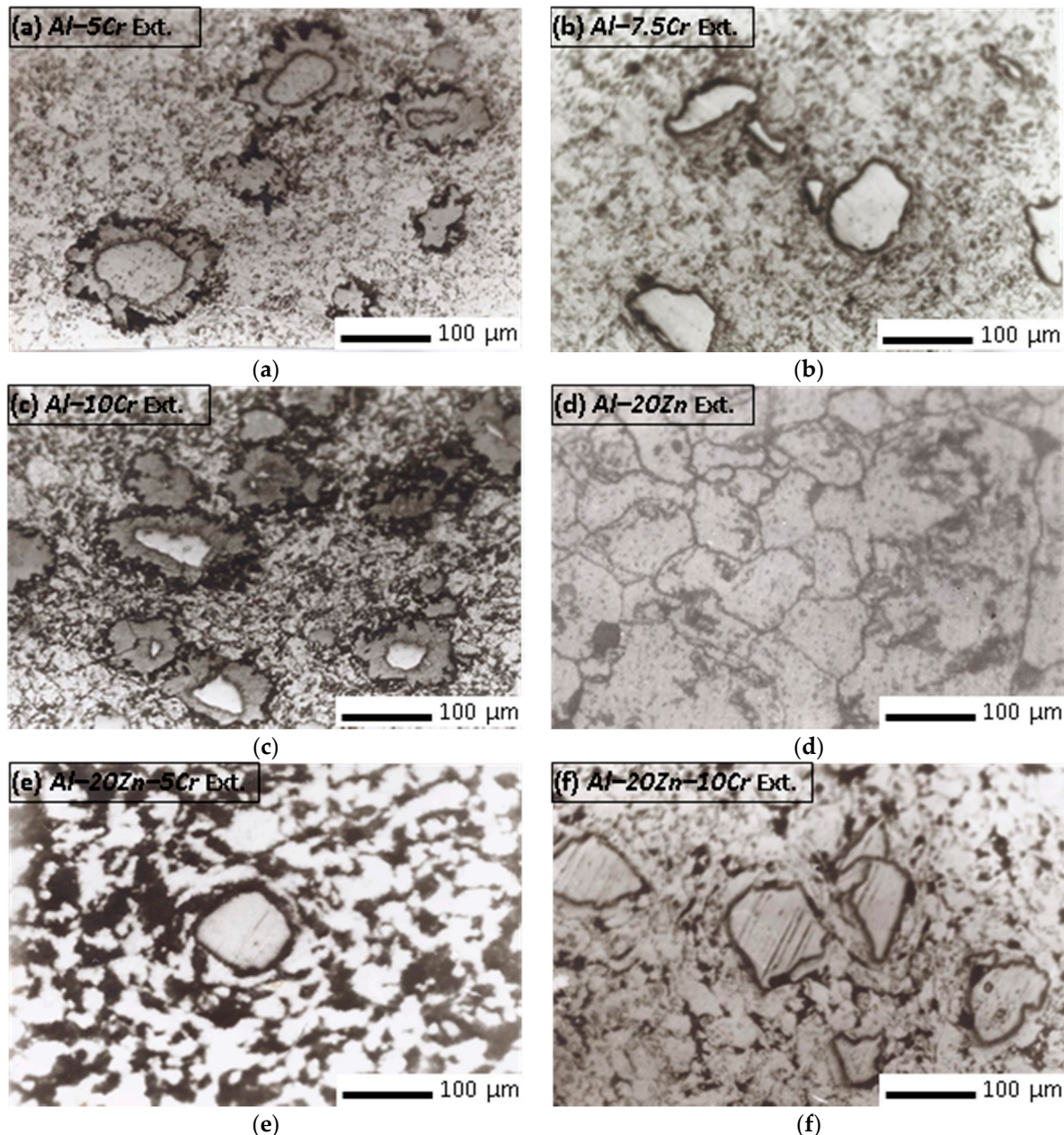


Figure 4. The microstructure of the different as extruded Al-based alloys.

3.4. Mechanical Properties

Tensile specimens were prepared from the heat treated materials, and as extruded states. The gauge length and gauge diameter of the specimens were 30mm and 6 mm respectively. Tensile tests were performed at a cross head speed of 2.0 mm/min, which corresponded to an initial strain rate of $1.1 \times 10^{-3} \text{ s}^{-1}$. Tensile tests were conducted at room temperature using materials testing system (MTS) testing machine (model 610) fitted with a 160 kN load cell operating in the displacement control mode under quasi static loading. The samples were deformed until crashed. For consistency and homogeneity assurance, three identical samples were prepared for each test case and exposed to the same loading conditions. The average test value of all the three samples of the radial crushing strength was reported in Table 1.

Table 1 presents the tensile properties of the materials in both as extruded state and the heat treated state. For the alloys Al-Cr without Zn, their ultimate tensile strength decreases with the increasing Cr amount and so does their tensile ductility. Comparing the tensile properties of the

materials containing Zn with the materials Zn free, one can see that the addition of Zn shows improving both the tensile strength and ductility of Al-20Zn-5Cr and Al-20Zn-10Cr alloys, in the as extruded state. Thus, the Zinc addition appears to be quite favorable as far as the mechanical properties are concerned. The heat treatment, applied to the zinc-containing alloys, does not improve their tensile ductility. This was probably related to an improved bonding between the matrix and the chromium as a result of the released local stresses around the chromium particles induced during extrusion.

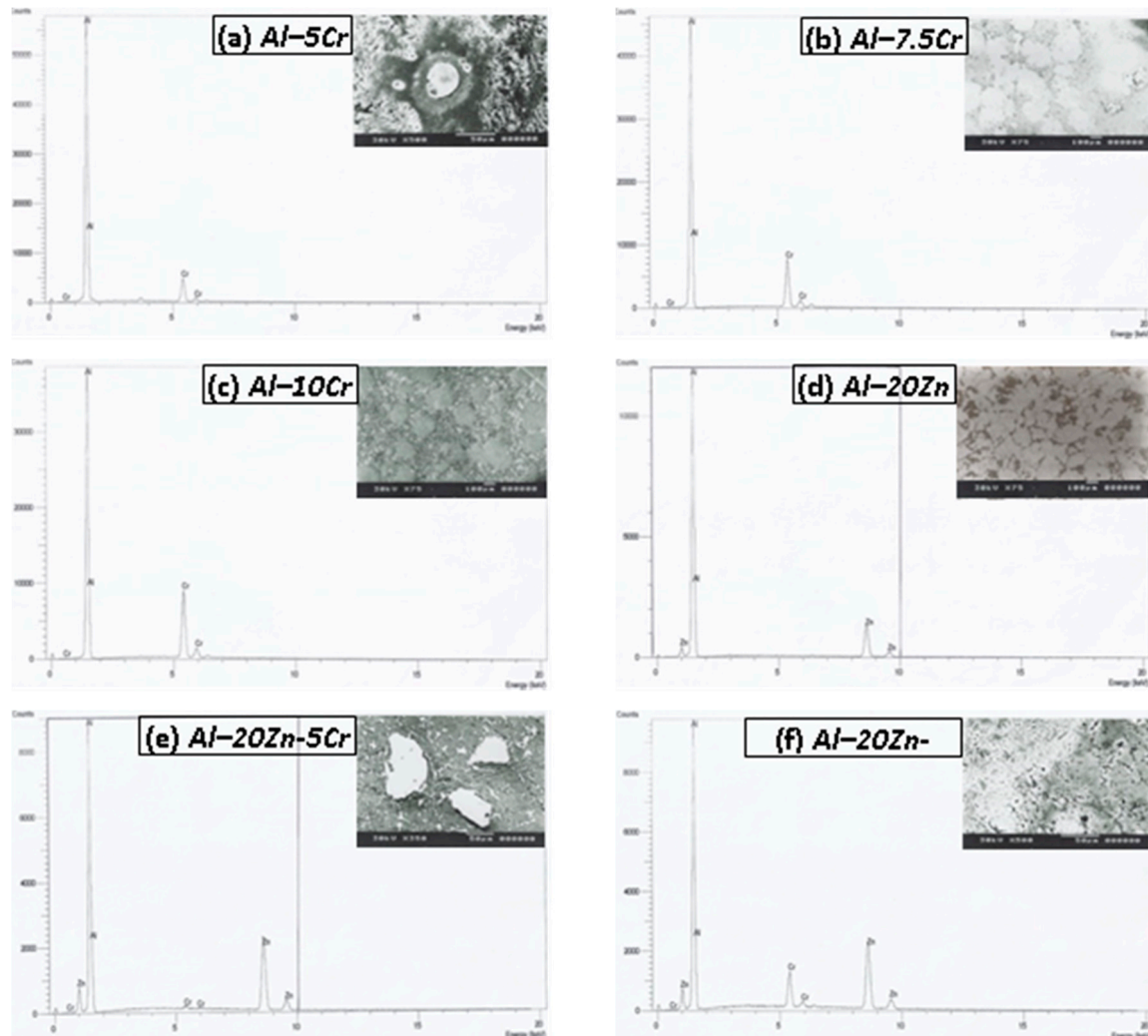


Figure 5. The EDX analysis at the indicated regions with higher magnification for the different Al-based alloys.

Table 1. Tensile data of Al-base alloys as extrusion and heat treatment.

Alloy Composition	As Extruded state		Heat treated state	
	UTS (σ_u) MPa	Fracture strain (ϵ_f) %	UTS (σ_u) MPa	Fracture strain (ϵ_f) %
Al-5Cr	75	12	105	10
Al-7.5Cr	70	10	101	8
Al-10Cr	65	8	96	6
Al-20Zn	188	18	185	16
Al-20Zn-5Cr	95	14	160	12
Al-20Zn-10Cr	80	10	143	8

Rockwell hardness measurements are performed for different produced materials using digital Rockwell hardness tester at 60 kg load (HRA-60). At least five readings were taken for each case and the average value was recorded to insure the consistency and homogeneity throughout the material surface. In all alloys the bright phase, which corresponds to δ -phase had Vickers hardness measurements about two times greater than the corresponding matrix as presented in Table 2.

Table 2. Rockwell hardness values Kg/mm² for the different Al-base alloys after extrusion and heat treatment.

Chemical Composition	Rockwell hardness As Extruded	Rockwell hardness Heat Treated at 500°C
Al-5Cr	8.9	9.0
Al-7.5Cr	9.5	12.5
Al-10Cr	9.9	14.6
Al-20Zn	10.4	27.6
Al-20Zn-5Cr	17.4	30.6
Al-20Zn-10Cr	16.9	32.1

The effect of heating temperatures on hardness for both as extruded and heat treatment of Al-base alloys were listed in Table 2. The heat treated Al-Zn-Cr alloys demonstrates improvement in hardness values comparing with specimen without heat treatment. The heat treatment Al-20Zn-5Cr alloys at 500°C had the highest hardness value of 40.8 that represents an increase in hardness of more than 35% compared to that of the specimen without heat treatment. On the other hand, the increase of Cr particles in the Al-base matrix results in decrease of hardness values as shown in Table 2. It should be noticed with the decrease of the aluminum content in the Al-based alloys, and the increase of the Cr, and Zn content the density increases accordingly.

3.5. Corrosion Rate

Corrosion rate were measured for the Al-based alloys using electrochemical polarization. The tests were performed in a corrosion cell that contained 250 ml of 3.5 wt.% NaCl solutions at room temperature and at a scan rate of 0.5 mV/s saturated air. All electrochemical measurements were conducted using a potentiostat AUTOLAB PGSTATE 30 and analyzed using Galvanostat M352 software at room temperature. Platinum gauze was used as a counter electrode and silver/silver chloride was the referenced. The exposed area was 1 cm² of all the heat treated and as extruded Al-based alloys.

An activation controlled cathodic process occurred in the cathodic branch, and the main reaction was hydrogen evolution during the measurements. As the applied potential increased, an activation controlled anodic process was observed. The electrochemical parameters such as polarization resistance (Rp) were measured. Corrosion current density (Icorr) was measured using the linear polarization resistance technique and obtained as a function of Rp, with β_c as the cathodic and β_a the anodic Tafel slopes, as $I_{corr} = \beta / R_p$, where β is a constant value and can be calculated by following equation:

$$\beta = \beta_c \beta_a / 2.3 (\beta_a + \beta_c) \tag{1}$$

The corrosion rate (C_R) expressed in mm per year was obtained from I_{corr} in air saturated 0.5N sodium chloride solution, according to the equation (2):

$$C_R = 0.13 I_{corr} (eq_{wt.}) / \rho \tag{2}$$

where $eq_{wt.}$ is the equivalent weight and ρ is density in g/cm^3 and I_{corr} is the corrosion current density determined by the linear polarization method using the Stern-Geary equation [24]. The corrosion parameters of Al-based alloys are presented in Table 3 for both as extruded and heat treated Al-based alloys.

Table 3. The electrochemical corrosion data for both as extruded and heat treated Al-based alloys.

Chemical Composition	As Extruded CR mm/year	Heat Treated at 500°C CR mm/year
Al pure	0.031	--
Al-5Cr	0.030	0.028
Al-7.5Cr	0.029	0.027
Al-10Cr	0.029	0.026
Al-20Zn	0.028	0.024
Al-20Zn-5Cr	0.026	0.022
Al-20Zn-10Cr	0.022	0.020

It is noticed that with increase of the Cr and Zn additives in the Al-based alloys the corrosion rate decreases, as the corrosion resistance increases. As Al-20Zn-10Cr alloys have corrosion rate of 30% less than pure aluminum, the heat treated Al-based alloys had approximately corrosion rate of 7% less than as extruded Al-based alloys. This makes the Al-based alloys with higher additives of Cr and Zn undergo localized corrosion rather than uniform corrosion.

3.6. Wear Resistance

The materials were also subjected to pin-on-disk wear tests under an unlubricated condition, in air and at room temperature. The counter face (the disk) was made of steel with a hardness of RC 32. Before each test, the disk surface was polished by standard metallographic procedure [4, 7, and 25]. The tests were made for different lengths of running times up to 20 minutes under a constant pressure applied of about 0.127 MPa. Weight loss was calculated using a precise digital analog weight balance (accuracy of $\pm 0.005g$). Results of the wear resistance for the different Al-based alloys compositions and heat treatment conditions are plotted in Figures 6, 7 and 8. Figure 6 show that increasing Cr content in the binary Al-Cr alloys for the extruded conditions improves the wear resistance. For heat treatment of these alloys at 500°C for one hour decreased the weight loss by about 1.5 times.

The microstructure shown in Figure 3(a) indicates that heat treatment of the binary Al-Cr alloys lead to diffusion of aluminum in the chromium particles resulting in gradual alloying of the Cr particle. It is possible that some Cr particles were dissolved in Al-based alloys, which caused the hardening of the alloy and, consequently, an increase of the wear resistance. In the ternary alloys of Al-Zn-Cr, the addition of Zn increases the weight loss for the alloys containing 5 or 10wt.% Cr as

shown in Figure 7. This effect was more pronounced for the alloys containing 5wt.% Cr. The weight loss of these alloys was about 2 times higher compared to the 10wt.% Cr ternary alloys. In the as extruded condition, the addition of Zn to the Al-Cr alloys results in higher degree of homogeneity in the microstructure, Figure 3(e, and f). However, Cr is a hard metal and is expected to improve wear resistance.

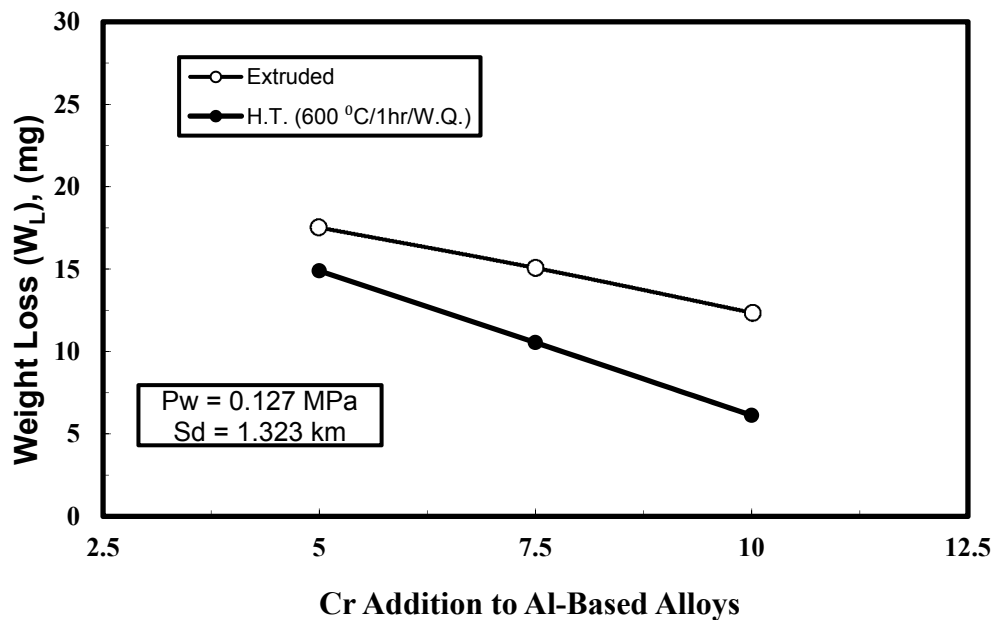


Figure 6. The effect of heat treatment on the weight loss for Al-Cr alloys.

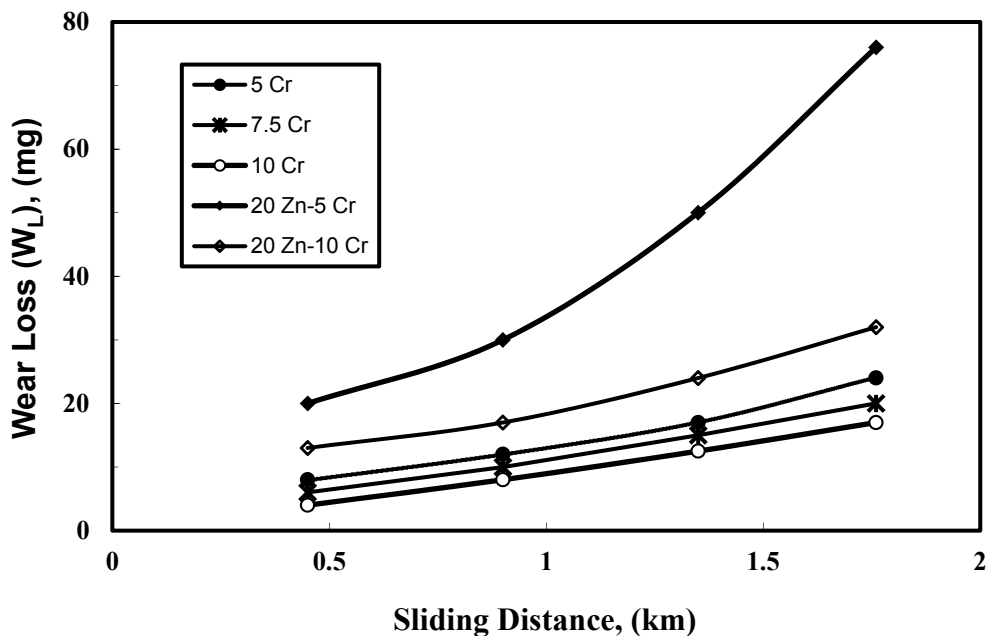


Figure 7. The weight loss versus sliding distance of Al-base alloys in the as extruded condition.

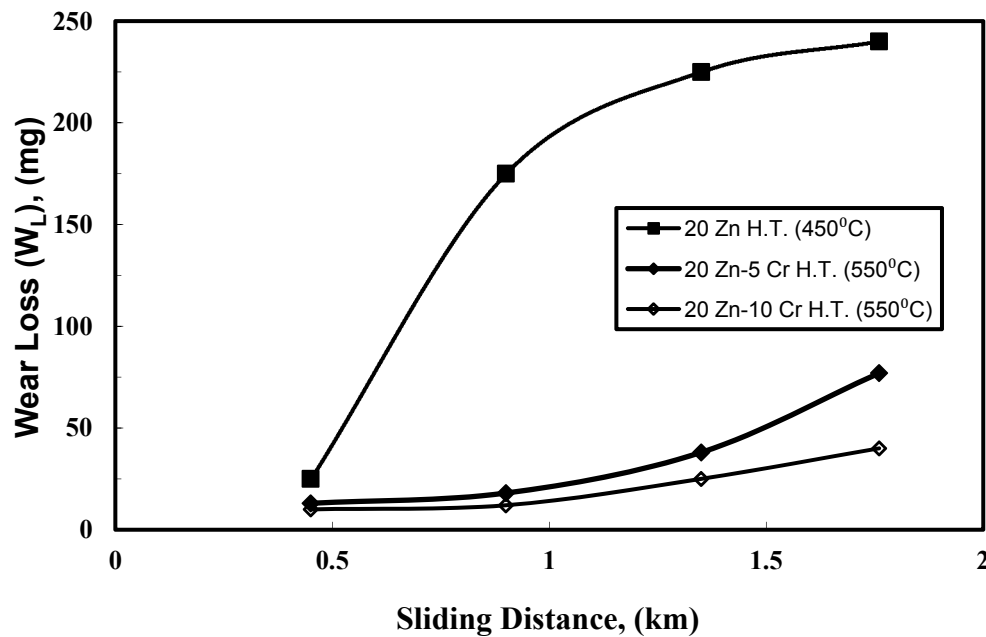


Figure 8. The effect of Cr addition on the weight loss of heat treated Al-20Zn alloys

The wear resistance results for the heat treated Al-20Zn alloys and Al-20Zn alloys containing 5 and 10wt.% Cr was plotted in Figure 8. The wear resistance of the Al-20Zn-Cr alloys were found to be around 5-8 fold greater than the Al-20Zn alloys after 1.76 km sliding distance. The presence of 20wt.% Zn in the Al-Cr alloys during heat treatment enhanced the inter-diffusion process and formation of homogenous Al-Zn-Cr alloys, Figure 3(e). The Cr particles have almost disappeared although EDX analysis (Figure 8 c and d) showed two phase alloys with different Cr contents. As mentioned above, the addition of Cr to the base alloy increased the hardness compared to the Al-20Zn alloys.

4. Conclusions

Based on the results of the present study, the following conclusions can be summarized:

1. Binary Al-Cr alloys from powders heat treated at different conditions could not establish homogenous microstructure.
2. The presence of 20wt.% Zn in the Al-Cr alloys enhanced the interdiffusion and densification process during heat treatment due to the formation of a liquid phase, which led to homogenizing the microstructure.
3. Both Zn addition and the heat treatment temperature affect the hardness values and the structure of the Al-base matrix
4. Under tension load, improvement in the strength for Al-Cr alloys was obtained after Zn addition and heat treatment process.
5. The increase of the Cr and Zn additives in the Al-based alloys the corrosion rate decreases, as the corrosion resistance increases. As Al-20Zn-10Cr alloys have corrosion rate of 30% less

than pure aluminum, the heat treated Al-based alloys had approximately corrosion rate of 7% less than as extruded Al-based alloys.

6. The wear resistance of the ternary Al-Zn-Cr heat treated at 500°C for one hour was about 5 times higher than that of the binary Al-Zn alloys. The alloy Al-20Zn-5Cr heat treated at 500°C for one hour followed by water quenching exhibited the highest wear resistance among the investigated alloys.

Author's contributions: All authors have equal contributions. Authors have no competing financial interests. The authors also declare no conflict of interest.

References

1. Liu, S.; Zhong, Q.; Zhang, Y.; Liu, W.; Zhang, X.; Deng, D. Investigation of quench sensitivity of high strength Al-Zn-Mg-Cu alloys by time-temperature-properties diagrams. *Mater. & Des.* **2010**, *31*, 3116–3120.
DOI: <http://dx.doi.org/10.1016/j.matdes.2009.12.038>
2. Ezuber, H.; El-Houd, A.; El-Shawesh, F. A study on the corrosion behavior of aluminum alloys in seawater. *Mater. & Des.* **2008**, *29*, 801–805.
DOI: <http://dx.doi.org/10.1016/j.matdes.2007.01.021>
3. Kalkanl, A.; Yilmaz, S. Synthesis and characterization of aluminum alloy 7075 reinforced with silicon carbide particulates. *Mater. & Des.* **2008**, *29*, 775–780.
DOI: <http://dx.doi.org/10.1016/j.matdes.2007.01.007>
4. Nassef, A.; El-Hadek, M. Mechanics of hot pressed aluminum composites. *Int. J. Adv. Manuf. Technol.* **2015**, *76*, 1905–1912.
DOI: <http://dx.doi.org/10.1007/s00170-014-6420-4>
5. El-Hadek, M.; Kassem, M. Failure behavior of Cu-Ti-Zr-based bulk metallic glass alloys. *J. Mater. Sci.* **2009**, *44*, 1127–1136.
DOI: <http://dx.doi.org/10.1007/s10853-008-3194-9>
6. El-Hadek, M.; Kaytbay, S. Al₂O₃ Particle Size Effect on Reinforced Copper Alloys: An Experimental Study. *Strain.* **2009**, *45*, 506–515.
DOI: <http://dx.doi.org/10.1111/j.1475-1305.2008.00552.x>
7. Nassef, A.; El-Hadek, M. Microstructure and Mechanical Behavior of Hot Pressed Cu-Sn Powder Alloys. *Adv. Mater. Sci. Eng.* **2016**, *2016*, 1–10.
DOI: <http://dx.doi.org/10.1155/2016/9796169>
8. Kurtuldu, G.; Jarry, P.; Rappaz, M. Influence of Cr on the nucleation of primary Al and formation of twinned dendrites in Al-Zn-Cr alloys: Can icosahedral solid clusters play a role?. *Acta. Mater.* **2013**, *61*, 7098–7108.
DOI: <http://dx.doi.org/10.1016/j.actamat.2013.07.056>
9. Kurtuldu, G.; Jarry, P.; Rappaz, M. Influence of icosahedral short range order on diffusion in liquids: A study on Al-Zn-Cr alloys. *Acta Materialia* **2016**, *115*, 423–433.
DOI: S1359645416304128
10. del Arco, M.; Rives, V.; Trujillano, R.; Malet, P. Thermal behavior of Zn-Cr layered double hydroxides with hydrotalcite-like structures containing carbonate or decavanadate. *J. Mater. Chem.* **1996**, *6*, 1419–1428.
DOI: <http://dx.doi.org/10.1039/JM9960601419>
11. Peng, G.; Chen, K.; Fang, H.; Chen, S. Effect of Cr and Yb additions on microstructure and properties of low copper Al-Zn-Mg-Cu-Zr alloy. *Mater. & Des.* **2012**, *36*, 279–283.
DOI: <http://dx.doi.org/10.1016/j.matdes.2011.11.040>
12. He, Z.; Su, X.; Peng, H.; Liu, L.; Wu, C.; Wang, J. 600 °C isothermal section of the Al-Cr-Zn ternary phase diagram. *Journal of Alloys and Compounds* **2015**, *649*, 1239–1245.
DOI: S0925838815306332
13. Li, C.B.; Han, S.Q.; Liu, S.D.; Deng, Y.L.; Zhang, X.M. Grain structure effect on quench sensitivity of Al-Zn-Mg-Cu-Cr alloy. *Trans. Nonferrous Met. Soc. China* **2016**, *26*, 2276–2282.
DOI: S1003632616643194
14. Fourmentin, R. Avettand-Fènoël, M. N.; Reumont, G.; Perrot, P. The Fe-Zn-Al-Cr system and its impact on the galvanizing process in chromium-added zinc baths. *J. Mater. Sci.* **2008**, *43*, 6872–6880.
DOI: <http://dx.doi.org/10.1007/s10853-008-3011-5>

15. Shaha, S.K.; Czerwinski, F.; Kasprzak, W.; Friedman, J.; Chen, D.L. Ageing characteristics and high-temperature tensile properties of Al–Si–Cu–Mg alloys with micro-additions of Cr, Ti, V and Zr. *Mater. Sci. Eng., A* **2016**, *652*, 353–364.
DOI: S0921509315306389
16. Shin, Sang-S.; Lim, Kyung-M.; Park, Ik-M. Effects of high Zn content on the microstructure and mechanical properties of Al–Zn–Cu gravity-cast alloys. *Mater. Sci. Eng., A* **2017**, *679*, 340–349.
DOI: S1002007114000264
17. Chinh, N.Q.; Jenei, P.; Gubicza, J.; Bobruk, E.V.; Valiev, R. Z.; Langdon, T. G. Influence of Zn content on the microstructure and mechanical performance of ultrafine-grained Al–Zn alloys processed by high-pressure torsion. *Materials Letters* **2017**, *186*, 334–337.
DOI: S0167577X16315749
18. Staišius, L.; Miečinskas, P.; Leinartas, K.; Selskis, A.; Grigucevičienė, A.; Juzeliūnas, E. Sputter-deposited Mg–Al–Zn–Cr alloys–Electrochemical characterization of single films and multilayer protection of AZ31 magnesium alloy. *J. Corros. Sci.* **2014**, *80*, 487–493.
DOI: <http://dx.doi.org/10.1016/j.corsci.2013.11.061>
19. Wang, H.; Zhang, R.; Hu, X.; Wang, C.A.; Huang, Y. Characterization of a powder metallurgy SiC/Cu–Al composite. *J. Mater. Process. Technol.* **2008**, *197*, 43–48.
DOI: <http://dx.doi.org/10.1016/j.jmatprotec.2007.06.002>
20. Ogel, B.; Gurbuz, R. Microstructural characterization and tensile properties of hot pressed Al–SiC composites prepared from pure Al and Cu powders. *Mater. Sci. Eng., A* **2001**, *301*, 213–220.
DOI: [http://dx.doi.org/10.1016/S0921-5093\(00\)01656-7](http://dx.doi.org/10.1016/S0921-5093(00)01656-7)
21. Chang, Y.; Sun, W.; Xiong, X.; Chen, Z.; Wang, Y.; Hao, Z.; Xu, Y. A novel design of Al–Cr alloy surface sealing for ablation resistant C/C–ZrC–SiC composite. *Journal of the European Ceramic Society*, **2017**, *37*, 859–864.
DOI: S0955221916304812
22. El-Hadek, M.; Kassem, M. Characterization of strengthened rapidly quenched Zr-based alloys. *Int. J. Mech. Mater. Des.* **2008**, *4*, 279–289.
DOI: <http://dx.doi.org/10.1007/s10999-008-9068-0>
23. El-Hadek, M.; Kaytbay, S. Fracture properties of SPS tungsten copper powder composites. *Metall. Mater. Trans. A* **2013**, *44*, 544–551.
DOI: <http://dx.doi.org/10.1007/s11661-012-1396-x>
24. Ozyilmaz, A.T.; Kardas, G.; Erbil, M.; Yazici, B. The corrosion performance of polyaniline on nickel plated mild steel. *Appl. Surf. Sci.* **2005**, *242*, 97–106.
DOI: <http://dx.doi.org/10.1016/j.apsusc.2004.08.002>
25. Kaytbay, S.; El-Hadek, M. Wear resistance and fracture mechanics of WC–Co composites. *Int. J. Mater. Res.* **2014**, *105*, 557–565.
DOI: <http://dx.doi.org/10.3139/146.111069>



© 2017 by the authors. Licensee *Preprints*, Basel, Switzerland. This article is an open access article distributed under the terms and conditions of the Creative Commons by Attribution (CC-BY) license (<http://creativecommons.org/licenses/by/4.0/>).